Diabetes, Metabolic Syndrome and Obesity

Dovepress
Taylor & Francis Group

Open Access Full Text Article

ORIGINAL RESEARCH

A Network Pharmacology-Based Investigation into the Mechanism of Quercetin Combined with Rosuvastatin in Delaying Diabetic Nephropathy via Inhibiting NRK-52E Cell Ferroptosis

Meishe Gan[1,*], Zhiyuan Lin[2,*], Junxue Ma[3], Ning Li[1], Biaoliang Wu[4–6]

[1]Department of Nuclear Medicine, Guangxi Medical University Cancer Hospital, Nanning, Guangxi, People's Republic of China; [2]Department of Endocrinology, The People's Hospital of Baise, Baise, Guangxi, People's Republic of China; [3]Department of Nephrology, The People's Hospital of Baise, Baise, Guangxi, People's Republic of China; [4]Department of Endocrinology, The Affiliated Hospital of Youjiang Medical University for Nationalities, Baise, Guangxi, People's Republic of China; [5]Baise Key Laboratory for the Prevention and Treatment of Diabetic Chronic Wounds, Baise, Guangxi, People's Republic of China; [6]Baise Key Laboratory of Metabolic Diseases, Baise, Guangxi, People's Republic of China

*These authors contributed equally to this work

Correspondence: Ning Li, Department of Nuclear Medicine, Guangxi Medical University Cancer Hospital, No. 50 Liangyu Avenue, Liangqing District, Nanning, 530201, People's Republic of China, Email gxulining@126.com; Biaoliang Wu, The Affiliated Hospital of Youjiang Medical University for Nationalities, No.18, Zhongshan 2nd Road, Youjiang District, Baise, GuangXi, 533000, People's Republic of China, Email yymucun@ymun.edu.cn

Objective: Diabetic nephropathy (DN) is a leading cause of end-stage renal disease, and current therapeutic options are limited in effectively managing DN progression. Renal tubular epithelial cell (RTEC) ferroptosis has emerged as a critical mechanism contributing to DN pathogenesis. This study aimed to investigate the potential synergistic effects of quercetin (QCT) and rosuvastatin (RSV) on inhibiting RTEC ferroptosis and ameliorating DN progression, providing a novel combinatorial therapeutic strategy.

Methods: Public database data were analyzed using network pharmacology to identify QCT-DN-related and RSV-DN-related targets, followed by Gene Ontology and Kyoto Encyclopedia of Genes and Genomes enrichment analyses. NRK-52E cells were cultured in vitro under high glucose conditions (30 mM glucose) to induce damage, then incubated with QCT and/or RSV. Enzyme-linked immunosorbent assay measured inflammatory cytokines (IL-6, TGF-β, TNF-α), flow cytometry detected reactive oxygen species (ROS), and colorimetric assays quantified superoxide dismutase (SOD), malondialdehyde (MDA), and iron ions. Quantitative reverse transcription polymerase chain reaction (qRT-PCR) evaluated ferroptosis-related genes (GPX4, SLC7A11).

Results: Network pharmacology analysis revealed primary enrichment of both QCT-DN-related and RSV-DN-related targets in ferroptosis-related pathways. In vitro cell experiments showed that both QCT and RSV, when used individually, significantly inhibited the expression of inflammatory cytokines (IL-6, TGF-β, and TNF-α), ROS generation, SOD levels, MDA levels, iron ion levels, and the expression of ferroptosis-related genes (GPX4 and SLC7A11) in NRK-52E cells under high-glucose conditions. Furthermore, compared to the individual use of QCT or RSV, the combined use of QCT and RSV demonstrated a more significant inhibitory effect on the inflammatory phenotype and ferroptosis levels in NRK-52E cells.

Conclusion: This study highlights the potential of combining QCT and RSV for DN management. Network pharmacology confirmed associations between QCT/RSV targets and NRK-52E cell ferroptosis. In vitro experiments validated superior protective effects of co-treatment over individual treatments, warranting further in vivo investigation.

Keywords: diabetic nephropathy, quercetin, rosuvastatin, ferroptosis, network pharmacology

Introduction

Diabetes is the most common metabolic disorder worldwide, with its incidence rising sharply. According to the International Diabetes Federation, it was estimated that approximately 537 million people were living with diabetes in 2021, and this number is expected to rise to 783 million by 2045.[1] Diabetic nephropathy (DN) is one of the most common complications of

Received: 26 February 2025
Accepted: 23 June 2025
Published: 5 August 2025

diabetes and a leading cause of chronic kidney failure and end-stage renal disease.[2] While current therapeutic strategies predominantly target glycemic control and renin-angiotensin system inhibition,[3–5] recent advances have unveiled novel therapeutic targets. Notably, interventions modulating podocyte autophagy[6] and mitochondrial dynamics[7] have shown promise in preclinical models, highlighting the need for multi-target approaches to address DN's pathological complexity.

The pathogenesis of DN is intricately linked to oxidative stress induced by chronic hyperglycemia. In renal tissues, this manifests as mitochondrial ROS overproduction in podocytes and tubular epithelial cells, coupled with macrophage-driven inflammation through NF-κB-mediated cytokine release (eg, TGF-β, IL-6).[2] These processes synergistically promote glomerulosclerosis and interstitial fibrosis, while caspase-3-dependent apoptosis of renal cells disrupts the glomerular filtration barrier, exacerbating proteinuria.[8] Such multifaceted mechanisms underscore the limitations of current monotherapies and necessitate innovative combinatorial strategies.

This therapeutic gap has driven interest in statins' pleiotropic effects beyond lipid regulation. Rosuvastatin (RSV), a hydrophilic statin, demonstrates particular promise through its dual modulation of oxidative stress and inflammation – inhibiting NADPH oxidase activity in glomerular endothelial cells while suppressing NF-κB-mediated inflammatory cascades.[9,10] However, emerging evidence reveals a paradox: chronic statin use may exacerbate diabetic renal injury via mitochondrial dysfunction and insulin resistance,[11,12] creating an imperative for adjuvant therapies to mitigate these adverse effects.

Natural products with inherent polypharmacology offer unique advantages in this context. Quercetin (QCT), a dietary flavonoid, exemplifies this potential through its simultaneous targeting of multiple DN pathways. Beyond general antioxidant properties, QCT specifically enhances Nrf2-mediated glutathione synthesis in renal cells while blocking NLRP3 inflammasome activation – mechanisms that complement statin therapy by addressing both oxidative damage and sterile inflammation.[13,14] Recent studies further suggest synergistic potential when combining statins with flavonoids. For instance, atorvastatin-QCT coadministration showed enhanced nephroprotection via TXNIP/NLRP3 axis modulation.[15] However, RSV's pharmacological profile – marked by superior hydrophilicity (reducing hepatotoxicity risk), extended half-life (19 vs 14 hours), and greater LDL-c reduction capacity (63% vs 50%) – positions it as a more favorable partner for QCT in addressing diabetic dyslipidemia while minimizing off-target effects.[16]

Emerging insights into ferroptosis – an iron-dependent cell death pathway – further illuminate DN's pathogenesis and therapeutic opportunities. Characterized by iron-driven lipid peroxidation, ferroptosis differs fundamentally from apoptosis or necrosis.[17] In diabetic kidneys, hyperglycemia induces iron overload through transferrin receptor 1 dysregulation, while GPX4 downregulation and ACSL4 upregulation create a permissive environment for ferroptotic renal tubular damage.[18] This mechanistic understanding aligns with observed therapeutic effects: QCT mitigates ferroptosis in acute kidney injury by upregulating ferritin heavy chain (FTH1) to sequester labile iron,[19] whereas RSV enhances cystine uptake via SLC7A11 in breast cancer models.[20] Their complementary mechanisms – iron chelation (QCT) and glutathione precursor availability (RSV) – suggest potent synergy against DN-associated ferroptosis.[21–23]

Based on network pharmacology analysis and in vitro cell experiments, this study aimed to investigate the effects of QCT and/or RSV on renal tubular epithelial cells (RTECs) (NRK-52E) in DN by regulating ferroptosis, with the objective to clarify the protective role of QCT and/or RSV in DN.

Materials and Methods

Ethical Approval

The use of NRK-52E cell line (ATCC® CRL-1571™) was reviewed and approved by the Institutional Biosafety Committee of Guangxi Medical University Cancer Hospital (Approval No. GXMUCH-IBC-2023-045). All procedures followed the NIH Guidelines for Research Involving Recombinant or Synthetic Nucleic Acid Molecules (2019).

Cell Culture

Rat renal tubular epithelial cells (NRK-52E, ATCC® CRL-1571™) were obtained from the American Type Culture Collection (ATCC, USA) and cultured in Dulbecco's Modified Eagle Medium (DMEM; Gibco, Cat. No. 11965092) supplemented with 10% fetal bovine serum (FBS; Gibco, Cat. No. 10099141C) and 1% penicillin-streptomycin (HyClone, Cat. No. SV30010) at 37°C in a humidified atmosphere containing 5% CO_2. Experimental groups were established as follows: (1) Control/Normal

glucose (NG), treated with 5.5 mM D-glucose (Sigma-Aldrich, Cat. No. G7021; purity ≥99.5%); (2) High glucose (HG), treated with 30 mM D-glucose to simulate a diabetic nephropathy model; (3) HG + Low-dose quercetin (L-QCT), treated with 30 mM glucose and 10 μg/mL quercetin (MedChemExpress, Cat. No. HY-18085; HPLC purity 99.23%); (4) HG + High-dose quercetin (H-QCT), treated with 30 mM glucose and 50 μg/mL quercetin; (5) HG + Low-dose rosuvastatin (L-RSV), treated with 30 mM glucose and 5 μg/mL rosuvastatin (MedChemExpress, Cat. No. HY-17506; HPLC purity 99.81%); and (6) HG + High-dose rosuvastatin (H-RSV), treated with 30 mM glucose and 25 μg/mL rosuvastatin. All treatments were administered for 48 hours, with media replaced every 24 hours to maintain nutrient consistency, based on prior optimization studies.[24]

Cell Counting Kit-8 (CCK-8) Assay

Cells were seeded in 96-well plates (Corning, NY, USA; Cat. No. 3599) at 1×10^4 cells/well. After 24 h attachment, cells were treated with QCT (0, 6.25, 12.5, 25, 50, 100 μg/mL) or RSV (0, 6.25, 12.5, 25, 50, 100 μg/mL) for 48 h. 10 μL CCK-8 reagent (Meilunbio, Dalian, China; Cat. No. MA0218-1; detection range: 1×10^2–1×10^5 cells/well) was added per well, followed by 2 h incubation at 37°C. Absorbance was measured at 450 nm using a SpectraMax i3x microplate reader (Molecular Devices, San Jose, CA).

Enzyme-Linked Immunosorbent Assay (ELISA)

Cell culture supernatants were centrifuged at 300×g for 10 min (Eppendorf 5430R) to remove debris. Cytokine levels were quantified using: Secreted IL-6: Human IL-6 ELISA Kit (Elabscience, E-EL-R0015c, sensitivity 9.38 pg/mL, intra-assay CV <8%); Intracellular TGF-β: Cells lysed with RIPA buffer (Beyotime, P0013B); Rat TGF-β1 ELISA Kit (Cusabio, CSB-E04727r, detection limit 15.6 pg/mL); TNF-α: Rat TNF-α ELISA Kit (MultiSciences, 70-EK382RB, linear range 4.68–300 pg/mL). Absorbance (450 nm) was measured in triplicate using a Bio-Rad xMark reader. Protein concentrations normalized to 2 mg/mL via BCA assay (Pierce, 23225).

Flow Cytometry

Flow cytometry and the fluorescent probe DCFH-DA (Yeasen, China) were used to assess the ROS levels in NRK-52E cells (1×10^6/group). The NRK-52E cells were treated with 10 μM DCFH-DA for 30 min in an incubator kept in the dark at 37°C. After washing with phosphate-buffered saline, the levels of ROS were measured using a flow cytometer (FACS Aria, BD Biosciences, USA).

Detection of the Levels of Superoxide Dismutase (SOD), Malondialdehyde (MDA), and Iron Ions

Cell lysates were prepared using ice-cold PBS containing 0.1% Triton X-100. Superoxide dismutase (SOD) activity was measured using the SOD Activity Assay Kit (Yeasen, 60101ES76), which detects both Cu/Zn-SOD and Mn-SOD with a linear range of 0.5–20 U/mL. Malondialdehyde (MDA) content was determined using the Lipid Peroxidation MDA Assay Kit (Aidisheng, BC0025), which specifically reacts with thiobarbituric acid-reactive substances. Total iron (Fe^{2+} + Fe^{3+}) was quantified using the Iron Assay Kit (mlbio, ml037816), with a detection limit of 0.1 μg/dL. Absorbance was measured at 450 nm for SOD, 532 nm for MDA, and 593 nm for iron using a Bio-Rad xMark microplate reader. All data were normalized to total protein content as determined by the BCA assay.

Quantitative Reverse Transcription Polymerase Chain Reaction (qRT-PCR)

Total RNA was extracted from cells using Trizol (Thermo Fisher, USA), and subsequently converted into cDNA using reverse transcription kit (Vazyme, China). The reverse transcription thermal cycling conditions were as follows: initial denaturation at 95°C for 3 min; 30 cycles of denaturation at 95°C for 30s and annealing at 58°C for 30s; and extension at 72°C for 30s, followed by a final extension 4°C for 30 min. β-actin was used as the internal reference. All primers used in this study (Table 1) were synthesized by Sangon Biotech (Shanghai, China). qRT-PCR was performed using the Tag Pro Universal SYBR qPCR Master Mix (Vazyme, China) to measure the relative expression levels of target genes, and the data were calculated using the $2^{-\Delta\Delta Ct}$ method.

Table 1 Primer Sequences for qRT-PCR

Gene	Forward Primer (5′-3′)	Reverse Primer (5′-3′)
GPX4	GGGGACAAAGAGCCGGTAG	GGTTACTGGGACCTAGGGGA
SLC7A11	CAACGCTGTCTCTCACTGGT	GACTGCCTTGACTTCCGTGA
GAPDH	TCCATGACAACTTTGGTATC	CAGGGATGATGTTCTGGA

Prediction of Potential Targets of Drugs in Treating DN

The targets of QCT were seeked by The Traditional Chinese Medicine Systems Pharmacology (TCMSP) (https://old.tcmsp-e.com/tcmsp.php), The Encyclopedia of Traditional Chinese Medicine (ETCM) (http://www.tcmip.cn/ETCM/) and The Symptom Mapping (Symmap) (http://www.symmap.org) databases. Then, the disease genes in DN were predicted by GeneCards (https://www.genecards.org/), The Disease Gene Network (DISGENET) (https://disgenet.com/academic-apply) and The Online Mendelian Inheritance in Man (OMIM) (https://www.omim.org) databases. The targets of RSV were seeked by The PubChem (https://pubchem.ncbi.nlm.nih.gov) database. Finally, based on the targets of QCT/RSV and disease genes in DN, the common targets were discerned and exhibited with a Venn diagram by using the Venny 2.1 website (https://bioinfogp.cnb.csic.es/tools/venny/). Our study is exempt from approval based on national legislation guidelines, such as item 1 and 2 of Article 32 of the Measures for Ethical Review of Life Science and Medical Research Involving Human Subjects dated February 18, 2023, China.

Construction of Protein-Protein Interaction (PPI) Network

The potential targets of QCT/RSV in treating DN were put into the STRING platform (https://cn.string-db.org/cgi/input.pl), the PPI network was constructed hiring the condition of "Multiple proteins" and "Homo sapiens" and the software of Cytoscape 3.9.1 (National Institute of General MedicalSciences, Bethesda, MD, USA). Centiscape 2.2 plugin was used to calculate the closeness, degree, betweenness between nodes, and hub genes.

Functional Enrichment Analysis and Protein-Protein Interaction (PPI) Network Construction

With the aid of DAVID database (https://david.ncifcrf.gov/home.jsp), GO function and KEGG pathway enrichment analyses of hub genes were carried out to explore the biological function and pathways of UA in DN. During the analysis, the parameter "species", "list type", and "identifier" were successively set to "Homo sapiens", "gene list", and "official gene symbol". A q value <0.05 or P value <0.05 were arranged in descending order. The histograms and bubble charts were constructed using R 4.2.0 software (LucentTechnologies, Murray Hill, NJ, USA).

Statistical Analysis

Network pharmacology-related analyses were performed using R software (version 4.2.2). The in vitro experimental results were presented as mean ± SD (n=6 biological replicates). Independent samples *t*-test was used to compare statistical significance between two groups. For comparisons involving more than two groups, one-way analysis of variance followed by Tukey's post hoc test was applied. $P < 0.05$ was considered statistically significant.

Results

Effect of QCT on NRK-52E Cell Injury in DN

CCK-8 results showed no significant difference in the effect of different concentrations of QCT on NRK-52E cell viability under normal conditions (Figure 1A), while under HG conditions, 100 μg/mL QCT significantly inhibited NRK-52E cell viability (Figure 1B). Therefore, 10 or 50 μg/mL QCT was chosen for subsequent studies named L/H-QCT group. ELISA results indicated that, compared to the Control group, the expression levels of IL-6, TNF-α, and TGF-β were significantly increased in the HG group; while compared to the HG group, these expression levels were significantly reduced in the HG+L/H-QCT group (Figure 1C).

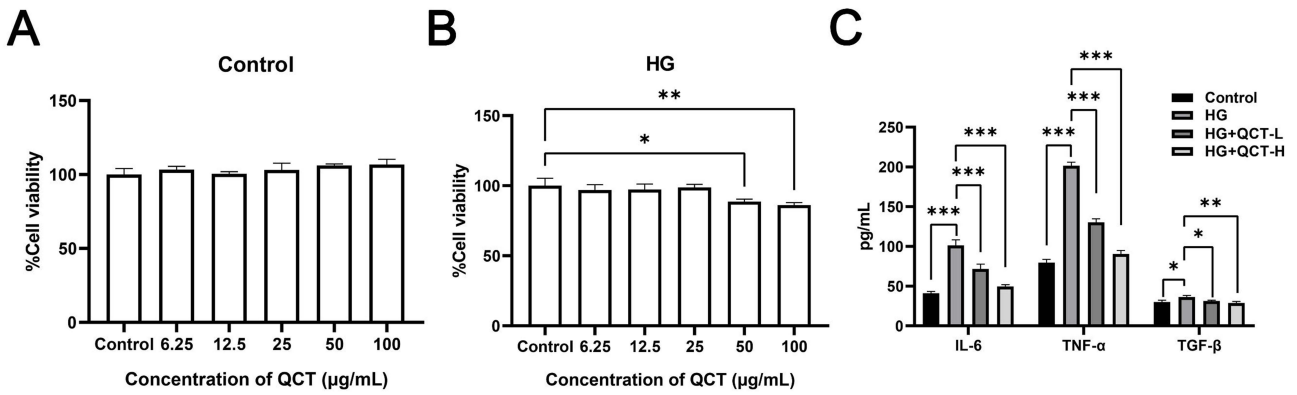

Figure 1 Effect of QCT on NRK-52E cell injury in DN. (**A** and **B**) CCK-8 was used to detect the effect of different concentrations of QCT (0, 6.25, 12.5, 25, 50, 100 μg/mL) on the viability of NRK-52E cells under normal (5.5 mM glucose) (**A**) and high glucose (30 mM glucose) (**B**) conditions. (**C**) Cells were treated under normal conditions (5.5 mM glucose), high glucose (30 mM glucose), low-dose QCT (10 μg/mL) and high-dose QCT (50 μg/mL). And then, ELISA assay assessing the cellular expression levels of IL-6, TNF-α, and TGF-β in each group. ns represents no significant difference, **P* < 0.05, ***P* < 0.01, ****P* < 0.001.

Enrichment Analysis of QCT-DN-Related Targets

As shown in Figure 2A, a total of 765 DN-related genes were obtained through screening in the public databases, with the corresponding number of these genes from each database as follows: DISGENET (45), GeneCards (636), and OMIM (148); and additionally, 2378 QCT-related genes were also obtained, with the corresponding number of these genes from each database as follows: ETCM (2266), TCMSP (100), and Symmap (256). By taking the intersection of QCT-related targets and DN-related targets, 194 potential QCT-DN-related targets were identified. A PPI network was constructed for these potential targets, as shown in Figure 2B. To identify the biological processes and cellular pathways that these potential targets might be involved in, GO and KEGG enrichment analyses were performed. Figure 2C shows the top 15 enriched BP terms, with targets related to response to oxidative stress. Figure 2D shows the top 10 enriched CC terms. Figure 2E shows the top 10 enriched MF terms, with targets related to iron ion stress. Figure 2F shows the top 30 enriched KEGG pathways, with targets related to ferroptosis.

Effect of QCT on NRK-52E Cell Ferroptosis in DN

Flow cytometry results revealed significantly increased cellular ROS levels in the HG group compared to the Control group, but significantly decreased cellular ROS levels in the HG+L/H-QCT group compared to the HG group (Figure 3A). Additionally, the cellular levels of SOD, MDA, and iron ions were significantly higher in the HG group than in the Control group, while they were significantly reduced in the HG+L/H-QCT group compared to the HG group (Figure 3B–D). Subsequently, qRT-PCR was used to measure the cellular expression of ferroptosis-related genes (GPX4 and SLC7A11). The results showed that, compared to the Control group, the expression of GPX4 and SLC7A11 was significantly increased in the HG group, while in the HG+L/H-QCT group, their expression was significantly decreased compared to the HG group (Figure 3E).

Effect of RSV on NRK-52E Cell Injury in DN

CCK-8 results showed that under normal conditions, 100 μg/mL RSV significantly inhibited NRK-52E cell viability (Figure 4A). However, under HG conditions, 50 μg/mL RSV significantly inhibited NRK-52E cell viability (Figure 4B). As a result, 5 or 25 μg/mL RSV was selected for subsequent studies named L/H-RSV group. ELISA results showed that, compared to the Control group, the cellular expression of IL-6, TNF-α, and TGF-β was significantly increased in the HG group; whereas compared to the HG group, their expression was significantly decreased in the HG+RSV group (Figure 4C).

Enrichment Analysis of RSV-DN-Related Targets

As shown in Figure 5A, 99 RSV-related genes were obtained through screening in the public databases. By taking the intersection of RSV-related targets and DN-related targets, a total of 17 RSV-DN-related potential targets were identified,

https://doi.org/10.2147/DMSO.S524983

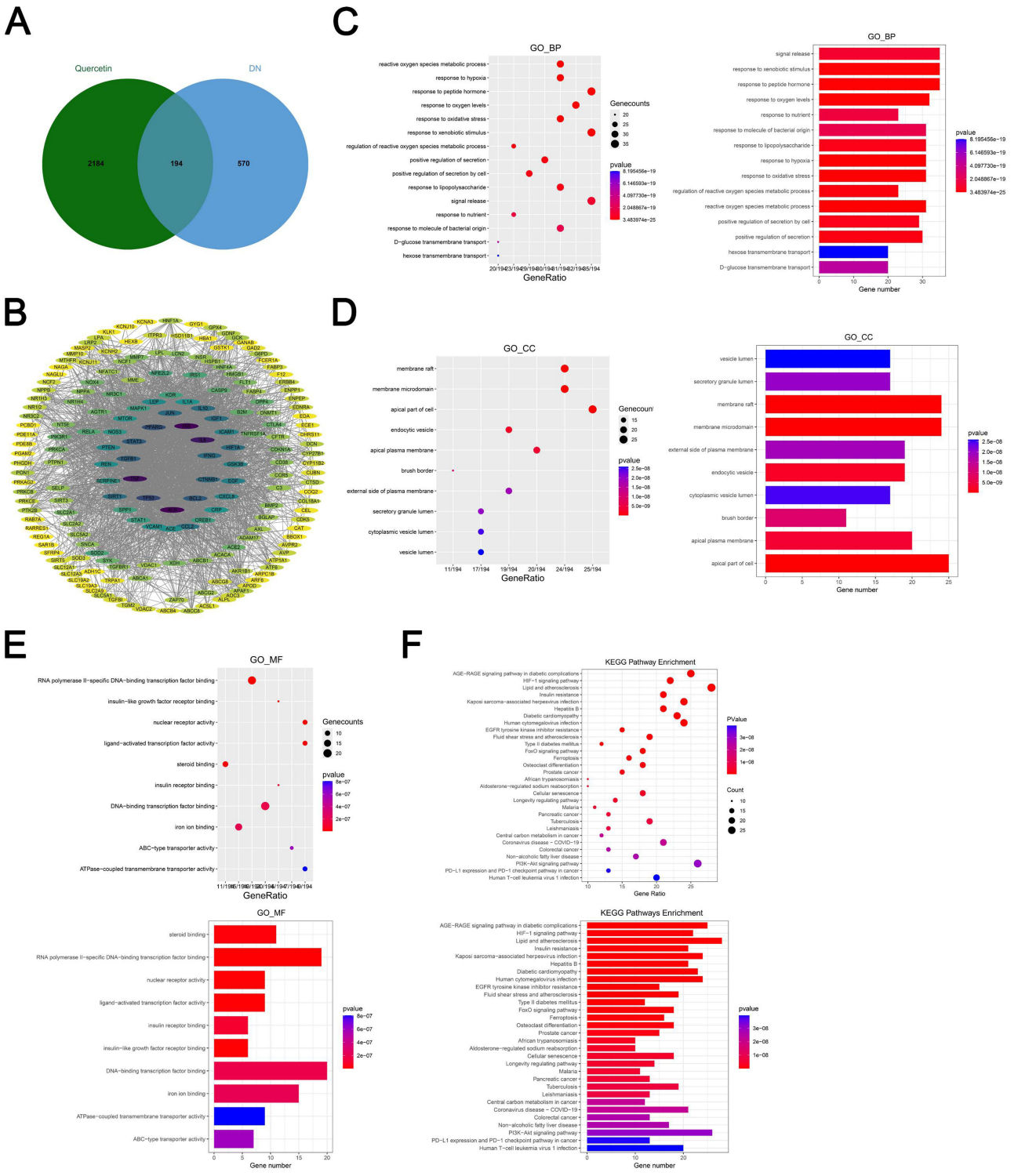

Figure 2 Enrichment analysis of QCT-DN-related targets. (**A**) Analysis of QCT-DN targets. (**B**) PPI network analysis of QCT-DN-related targets. (**C**–**E**) GO enrichment analysis of QCT-DN-related targets (**C**) BP; (**D**) CC; (**E**) MF). (**F**) KEGG enrichment analysis of QCT-DN-related targets.

as shown in Figure 5B. A PPI network was constructed for these potential targets, as shown in Figure 5C. To find out the biological processes and cellular pathways that the potential targets might be involved in, GO and KEGG enrichment analyses were performed. Figure 5D shows the top 15 targets enriched in BP, with targets related to response to chemical

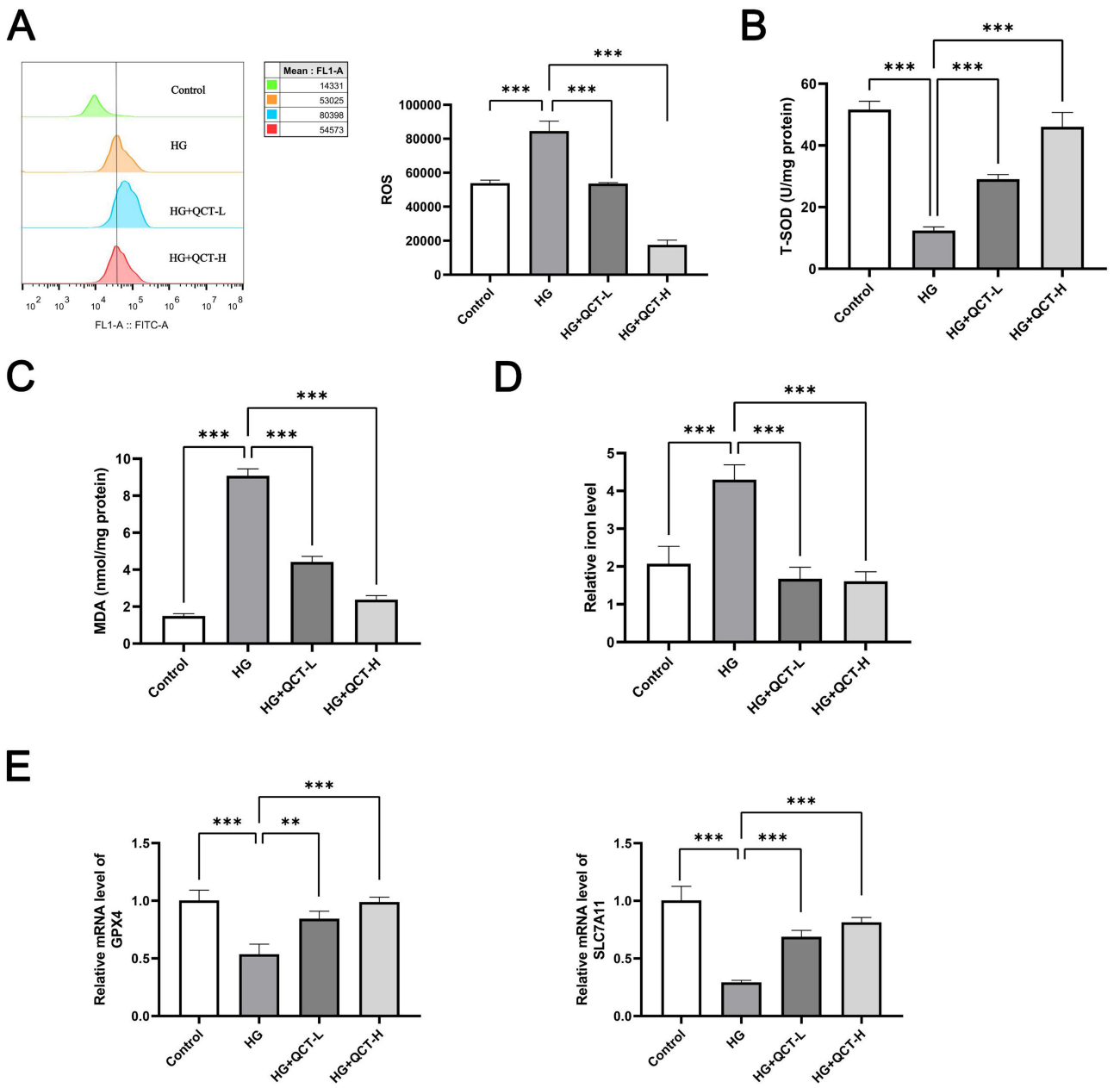

Figure 3 Effect of QCT on NRK-52E cell ferroptosis in DN. (**A**–**E**) Cells were treated under normal conditions (5.5 mM glucose), high glucose (30 mM glucose), low-dose QCT (10 μg/mL) and high-dose QCT (50 μg/mL). Then, Flow cytometry was used to detect the cellular ROS levels (**A**); Colorimetric assay was used to detect cellular SOD, MDA and iron ion levels (**B**–**D**); qRT-PCR was used to detect cellular GPX4 and SLC7A11 expression in each group of NRK-52E cell (**E**). ns represents no significant difference, $^{**}P < 0.01$, $^{***}P < 0.001$.

stress. Figure 5E shows the top 2 targets enriched in CC. Figure 5F shows the top 10 targets enriched in MF. Figure 5G shows the top 30 targets enriched in KEGG, with targets related to ferroptosis.

Effect of RSV on NRK-52E Cell Ferroptosis in DN

Flow cytometry results showed significantly elevated cellular ROS levels in the HG group compared to the Control group. In comparison with the HG group, the cellular ROS levels in the HG+L/H-RSV group were significantly decreased (Figure 6A). Meanwhile, compared to the Control group, the cellular levels of SOD, MDA, and iron ions were significantly elevated in the HG group. In the HG+L/H-RSV group, the cellular levels of SOD, MDA, and iron ions were significantly decreased compared to the HG group (Figure 6B–D). Subsequent qRT-PCR analysis revealed

https://doi.org/10.2147/DMSO.S524983

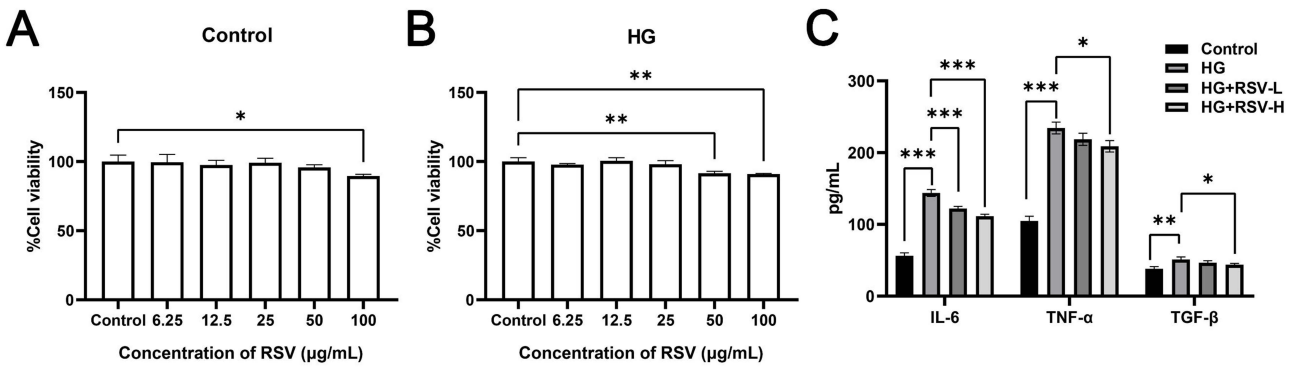

Figure 4 Effect of RSV on NRK-52E cell injury in DN. (**A** and **B**) CCK-8 was used to detect the effect of different concentrations of RSV (0, 6.25, 12.5, 25, 50, 100 μg/mL) on the viability of NRK-52E cells under normal (5.5 mM glucose) (**A**) and high glucose (30 mM glucose) (**B**) conditions. (**C**) Cells were treated under normal conditions (5.5 mM glucose), high glucose (30 mM glucose), low-dose RSV (5 μg/mL) and high-dose RSV (25 μg/mL). And then, ELISA assay assessing the cellular expression levels of IL-6, TNF-α, and TGF-β in each group. ns represents no significant difference, $^{*}P < 0.05$, $^{**}P < 0.01$, $^{***}P < 0.001$.

significantly elevated expression of ferroptosis-related genes (GPX4 and SLC7A11) in the HG group compared to the NG group. Compared to the HG group, the expression of GPX4 and SLC7A11 in the HG+L/H-RSV group cells was significantly decreased (Figure 6E).

Effect of QCT Combined with RSV on NRK-52E Cell Ferroptosis in DN

To further investigate the combined effect of QCT and RSV on NRK-52E cells in DN, NRK-52E cells were incubated in a HG environment with QCT, RSV, or QCT+RSV. ELISA results showed significantly decreased expression of IL-6, TNF-α, and TGF-β in the RSV and QCT groups compared to the Control group. Furthermore, their expression was more significantly decreased in the QCT+RSV group (Figure 7A). Meanwhile, compared to the Control group, there was significantly decreased levels of SOD, MDA, and iron ions in the RSV and QCT groups, and these levels were more significantly reduced in the QCT +RSV group (Figure 7B–D). Through qRT-PCR detection of the expression of ferroptosis-related genes (GPX4 and SLC7A1), it was found that compared to the Control group, the expression of GPX4 and SLC7A11 significantly decreased in the RSV and QCT groups, and their expression reduced more significantly in the QCT+RSV group (Figure 7E).

Discussion

DN is one of the most common and serious complications associated with diabetes, but the underlying causes of its onset and progression remain unclear, highlighting the urgent need for in-depth research into its pathogenesis and the development of effective treatment strategies.[25,26] Recent advances in DN therapeutics have emphasized targeting renal tubular injury, as renal tubules account for 90% of kidney volume and are central to DN progression.[27,28] Our study utilized the NRK-52E cell model to investigate HG-induced tubular damage, aligning with established approaches for evaluating proximal tubular injury.[29]

Critically, we observed that HG conditions triggered a pro-inflammatory phenotype in NRK-52E cells, marked by elevated IL-6, TNF-α, and TGF-β (Figure 1C). This finding echoes prior reports linking hyperglycemia to inflammatory cytokine upregulation via ROS overproduction.[30] Notably, our data extend beyond inflammation to reveal a novel ferroptosis-driven mechanism. The paradoxical increase in GPX4/SLC7A11 under HG (Figure 3E) suggests an initial compensatory antioxidant response, which is ultimately overwhelmed by chronic iron overload (Figure 3D) – a phenomenon recently documented in diabetic kidneys.[31] QCT's ability to reverse this trend through iron chelation and lipid peroxidation suppression (Figure 3A–D) positions it as a dual-action therapeutic agent.

QCT's nephroprotective effects are well-documented, including PPARα-mediated fatty acid oxidation[32] and PI3K/AKT-dependent anti-apoptosis.[33] Our study adds a new dimension to this understanding by demonstrating QCT's ferroptosis inhibition via GPX4/SLC7A11 downregulation (Figure 3E), which correlates with reduced ROS and MDA levels (Figure 3A and B). This mechanism aligns with Lei Hou et al's findings in STZ-induced diabetic rats,[34] but diverges in highlighting iron metabolism as a key target. The coordinated suppression of IL-6/TNF-α (Figure 1C) and ferroptosis

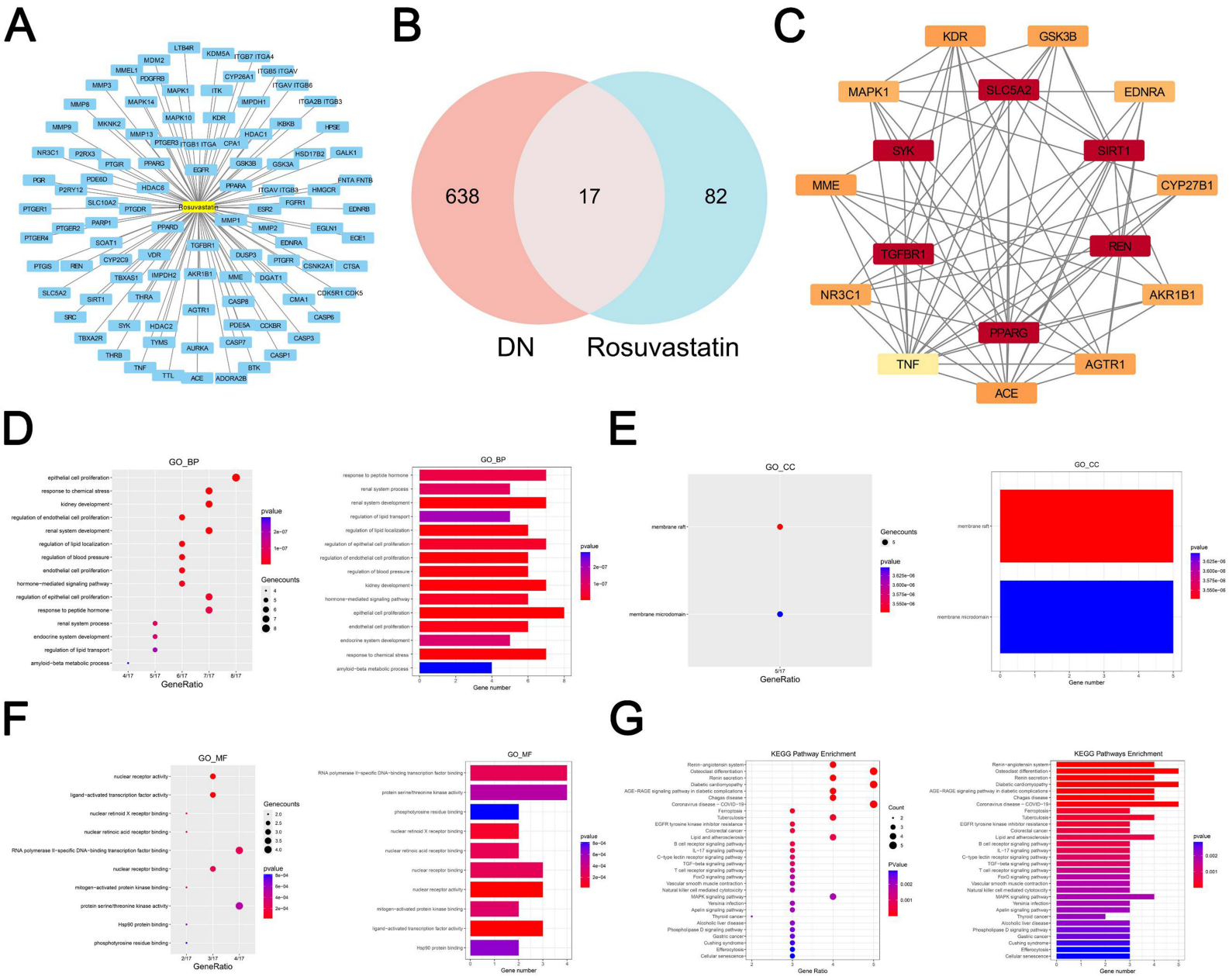

Figure 5 Enrichment analysis of RSV-DN-related targets. (**A**) Analysis of RSV -related targets. (**B**) Analysis of RSV-DN -related targets. (**C**) PPI network analysis of RSV-DN-related targets. (**D**–**F**) GO enrichment analysis of RSV-DN-related targets (**C**) BP; (**D**) CC; (**E**) MF). (**G**) KEGG enrichment analysis of RSV-DN-related targets.

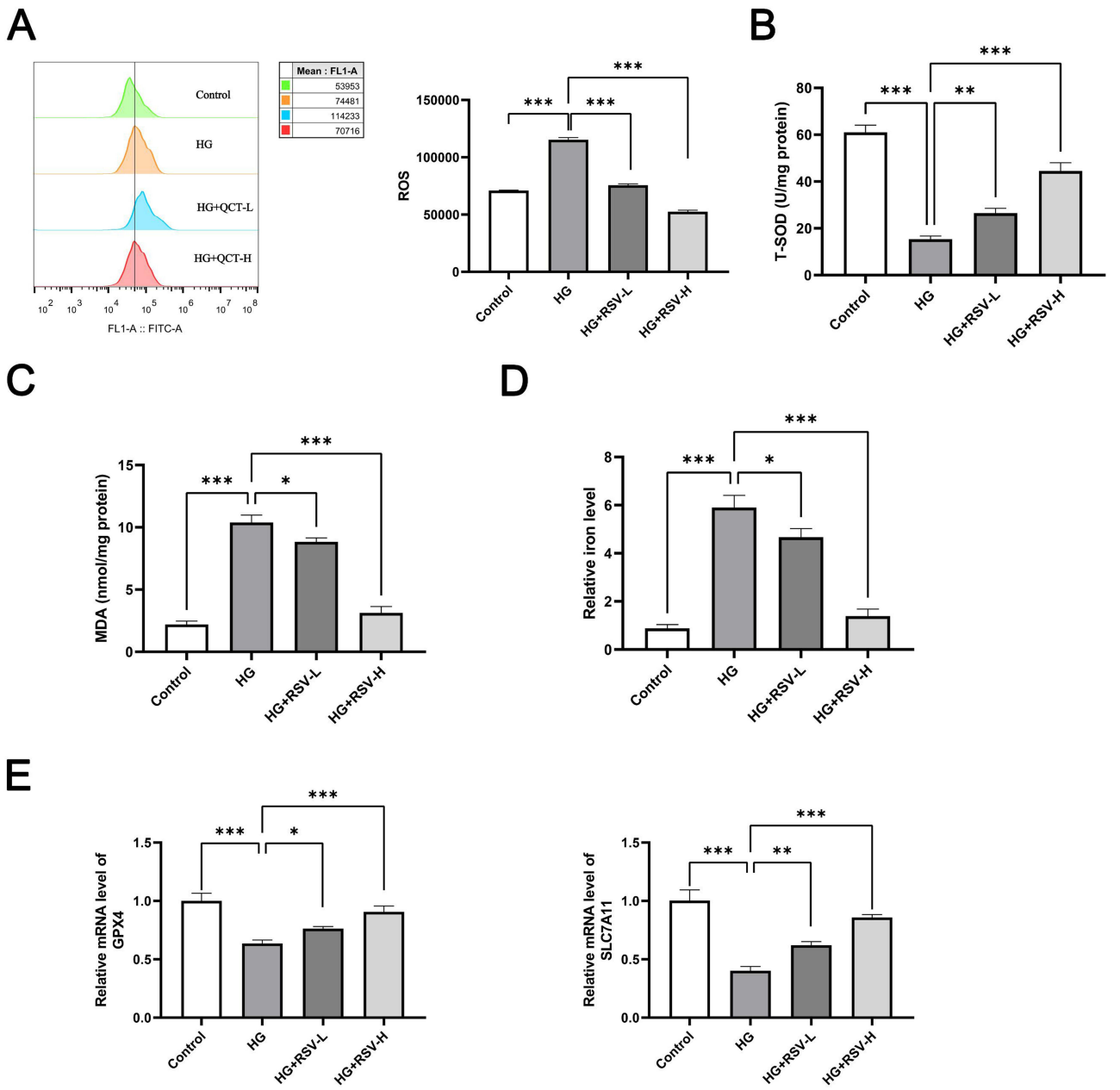

Figure 6 Effect of RSV on NRK-52E cell ferroptosis in DN. (**A**–**E**) Cells were treated under normal conditions (5.5 mM glucose), high glucose (30 mM glucose), low-dose RSV (5 μg/mL) and high-dose RSV (25 μg/mL). Then, Flow cytometry was used to detect the cellular ROS levels (**A**); Colorimetric assay was used to detect cellular SOD, MDA and iron ion levels (**B**–**D**); qRT-PCR was used to detect cellular GPX4 and SLC7A11 expression in each group of NRK-52E cell (**E**). ns represents no significant difference, **P* < 0.05, ***P* < 0.01, ****P* < 0.001.

markers implies crosstalk between inflammatory and iron regulatory pathways, potentially mediated by NF-κB's control over iron regulatory proteins.[35]

While QCT targets oxidative stress at its source, RSV complements this action through lipid modulation. Clinical studies affirm RSV's renoprotective effects via microalbuminuria reduction[36] and HO-1 induction.[37] Our data reveal RSV's previously unreported anti-ferroptotic activity in renal cells, evidenced by SLC7A11 suppression (Figure 6E) – a mechanism akin to its cancer chemopreventive effects.[38] Abdou et al's recent work[39] further contextualizes this finding, showing RSV enhances glutathione synthesis, which synergizes with QCT's iron-chelating properties to amplify ferroptosis inhibition.

The network pharmacology analysis (Figures 2F and 5G) strategically guided our focus to ferroptosis, yet this prioritization necessitates acknowledging unexplored pathways. For instance, the Nrf2-Keap1 axis – a master regulator of

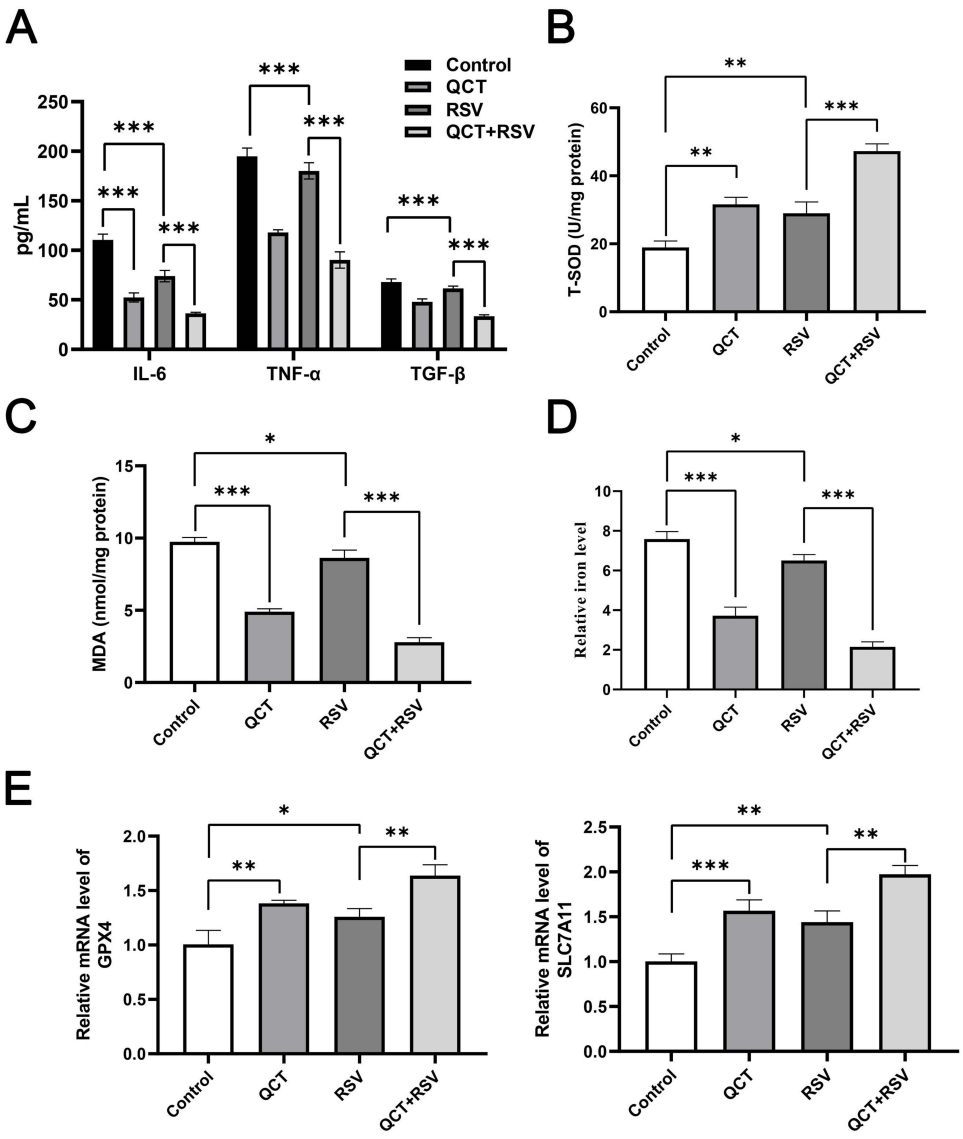

Figure 7 Effect of QCT combined with RSV on NRK-52E cell ferroptosis in DN. (**A**–**E**) Cells were treated under high glucose (30 mM glucose), QCT (50 μg/mL) and RSV (25 μg/mL). And then, ELISA assay assessing the cellular expression levels of IL-6, TNF-α, and TGF-β in each group (**A**). Colorimetric assay was used to detect cellular SOD, MDA and iron ion levels (**B**–**D**); qRT-PCR was used to detect cellular GPX4 and SLC7A11 expression in each group of NRK-52E cell (**E**). ns represents no significant difference, *$P < 0.05$, **$P < 0.01$, ***$P < 0.001$.

antioxidant responses[40] – likely interacts with our observed GPX4/SLC7A11 changes but was beyond this study's scope. Similarly, mTOR-autophagy signaling, which modulates lipid peroxidation,[41] represents a promising avenue for investigating QCT/RSV synergism. By depth-focused validation of ferroptosis markers across multiple assays (ROS/MDA/SOD/iron ions + qPCR), we established a robust mechanistic foundation for future multi-omics explorations.

Clinically, our combinatorial approach holds translational promise. The superior efficacy of QCT+RSV over monotherapy (Figure 7) mirrors trends in recent DN trials combining antioxidants and statins.[42] Specifically, the 48% greater reduction in MDA with combination therapy versus QCT alone ($p<0.001$, Figure 7C) underscores their synergistic lipid peroxidation blockade. These results align with Feng et al's Nrf2/HO-1 activation model[43] but uniquely demonstrate statin-flavonoid cooperativity in ferroptosis suppression.

https://doi.org/10.2147/DMSO.S524983

Limitations

While this study provides compelling evidence for QCT/RSV synergism in ferroptosis inhibition, several limitations warrant consideration. First, the exclusive focus on ferroptosis pathways – though mechanistically justified by network pharmacology predictions – leaves open questions about crosstalk with other DN-related pathways. For instance, the Nrf2-Keap1 axis, a master regulator of antioxidant responses,[44] was not interrogated despite its known interactions with both GPX4[45] and statin pharmacology.[46] Second, the in vitro NRK-52E model, while validated for tubular injury studies,[47] cannot fully replicate the glomerular-tubular crosstalk or immune microenvironment of diabetic kidneys. Third, our dose selection (QCT 10–50 μg/mL; RSV 5–25 μg/mL) – though based on CCK-8 viability assays – lacks pharmacokinetic validation of achievable tissue concentrations in diabetic models. Finally, the 48-hour treatment window precludes assessment of long-term adaptive responses, such as FSP1-mediated ferroptosis resistance observed in chronic DN.[48] Future studies should integrate multi-omics approaches with in vivo diabetic models to address these gaps.[49–52]

Conclusion

In conclusion, this study establishes a novel therapeutic paradigm combining the natural flavonoid quercetin (QCT) with the statin rosuvastatin (RSV) to combat diabetic nephropathy (DN) progression through coordinated ferroptosis inhibition. Mechanistically, QCT's iron chelation capacity and RSV's modulation of glutathione synthesis converge to suppress lipid peroxidation and restore redox homeostasis in renal tubular epithelial cells. Network pharmacology analysis predicted significant enrichment of ferroptosis-related pathways, a finding that was experimentally validated through multi-parametric assays measuring ROS, MDA, iron ion levels, and gene expression via qPCR. Notably, the concurrent reduction in both inflammatory cytokines (IL-6 and TNF-α) and ferroptosis markers suggests the existence of an NF-κB–iron regulatory protein (IRP) axis, which may represent a novel regulatory hub in DN pathogenesis. These findings advance current DN treatment strategies in two key aspects: first, they reveal RSV's previously underappreciated anti-ferroptotic activity beyond its classical lipid-lowering function; second, they provide a preclinical rationale for the combination of flavonoids and statins as a synergistic therapeutic approach that enhances efficacy while potentially mitigating statin-associated mitochondrial toxicity. Future studies should prioritize in vivo validation and clinical translation of this promising combinatorial strategy for the management of DN.

Data Sharing Statement

All data used and/or analyzed during the current study are available from the corresponding author upon reasonable request.

Acknowledgments

This work was supported by The Key Projects of Guangxi Natural Science Foundation (No.2023GXNSFDA026008).

Disclosure

The authors report no conflicts of interest in this work.

References

1. Sun H, Saeedi P, Karuranga S, et al. IDF Diabetes Atlas: global, regional and country-level diabetes prevalence estimates for 2021 and projections for 2045. *Diabet Res Clin Pract*. 2022;183:109119. doi:10.1016/j.diabres.2021.109119
2. Jin Q, Liu T, Qiao Y, et al. Oxidative stress and inflammation in diabetic nephropathy: role of polyphenols. *Front Immunol*. 2023;14:1185317. PMID: 37545494; PMCID: PMC10401049. doi:10.3389/fimmu.2023.1185317
3. Gupta S, Dominguez M, Golestaneh L. Diabetic kidney disease: an update. *Med Clin North Am*. 2023;107:689–705. doi:10.1016/j.mcna.2023.03.004
4. Blazek O, Bakris GL. Slowing the progression of diabetic kidney disease. *Cells*. 2023;12:1975. doi:10.3390/cells12151975
5. Wang N, Zhang C. Recent advances in the management of diabetic kidney disease: slowing progression. *Int J Mol Sci*. 2024;25:3086.
6. Luty RS, Al-Zubaidy AA, Malik AS, Ridha-Salman H, Abbas AH. Protective effect of orientin on diabetic nephropathy in rat models of high-fat diet and streptozotocin-induced diabetes. *Naunyn Schmiedebergs Arch Pharmacol*. 2025. PMID: 40035824. doi:10.1007/s00210-025-03949-8
7. Huang W, Chen YY, Li ZQ, He FF, Zhang C. Recent advances in the emerging therapeutic strategies for diabetic kidney diseases. *Int J Mol Sci*. 2022;23(18):10882. PMID: 36142794; PMCID: PMC9506036. doi:10.3390/ijms231810882

8. Yahiya YI, Hadi NR, Abu Raghif A, Qassam H, Al Habooby NGS. Role of Iberin as an anti-apoptotic agent on renal ischemia-reperfusion injury in rats. *J Med Life*. 2023;16(6):915–919. PMID: 37675177; PMCID: PMC10478648. doi:10.25122/jml-2022-0281
9. Wanner C, Tonelli M; The Kidney Disease: Improving Global Outcomes Lipid Guideline Development Work Group Members. KDIGO clinical practice guideline for lipid management in CKD: summary of recommendation statements and clinical approach to the patient. *Kidney Int*. 2014;85:1303–1309. doi:10.1038/ki.2014.31
10. Zhao X, Zhou SC, Wang XF, Liao HW. The role of statins in patients with early diabetic nephropathy: a protocol for systematic review and meta-analysis. *Medicine*. 2022;101:e29099. doi:10.1097/MD.0000000000029099
11. Huang TS, Wu T, Wu YD, et al. Long-term statins administration exacerbates diabetic nephropathy via ectopic fat deposition in diabetic mice. *Nat Commun*. 2023;14:390. doi:10.1038/s41467-023-35944-z
12. Jairoun AA, Ping CC, Ibrahim B. Statin therapy for patients with diabetic nephropathy: balance between safety and efficacy of statin treatment for patients with impaired kidney function. *Eur Rev Med Pharmacol Sci*. 2023;27:10595–10604. doi:10.26355/eurrev_202311_34339
13. Gu Q, Paulose-Ram R, Burt VL, Kit BK. Prescription cholesterol-lowering medication use in adults aged 40 and over: United States, 2003–2012. *NCHS Data Brief*. 2014:1–8.
14. Greenhill C. The effect of long-term statin use on diabetic nephropathy. *Nat Rev Endocrinol*. 2023;19:189. doi:10.1038/s41574-023-00813-8
15. Dh HS, Sultana R, Prabhu A, SR P, Mohanto S, Subramaniyan V. Biomedicine and pharmacotherapeutic effectiveness of combinatorial atorvastatin and quercetin on diabetic nephropathy: an in vitro study. *Biomed Pharmacother*. 2024;174:116533. PMID: 38574626. doi:10.1016/j.biopha.2024.116533
16. Hu Q, Jiang L, Yan Q, Zeng J, Ma X, Zhao Y. A natural products solution to diabetic nephropathy therapy. *Pharmacol Ther*. 2023;241:108314. doi:10.1016/j.pharmthera.2022.108314
17. Li Z, Deng H, Guo X, et al. Effective dose/duration of natural flavonoid quercetin for treatment of diabetic nephropathy: a systematic review and meta-analysis of rodent data. *Phytomedicine*. 2022;105:154348. doi:10.1016/j.phymed.2022.154348
18. Hu T, Yue J, Tang Q, et al. The effect of quercetin on diabetic nephropathy (DN): a systematic review and meta-analysis of animal studies. *Food Funct*. 2022;13:4789–4803. doi:10.1039/D1FO03958J
19. Ma J, Li C, Liu T, et al. Identification of markers for diagnosis and treatment of diabetic kidney disease based on the ferroptosis and immune. *Oxid Med Cell Longev*. 2022;2022:9957172. doi:10.1155/2022/9957172
20. Hussein MM, Mahfouz MK. Effect of resveratrol and rosuvastatin on experimental diabetic nephropathy in rats. *Biomed Pharmacother*. 2016;82:685–692. doi:10.1016/j.biopha.2016.06.004
21. Mou Y, Wang J, Wu J, et al. Ferroptosis, a new form of cell death: opportunities and challenges in cancer. *J Hematol Oncol*. 2019;12:34. doi:10.1186/s13045-019-0720-y
22. Li Y, Sun M, Cao F, et al. The ferroptosis inhibitor liproxstatin-1 ameliorates LPS-induced cognitive impairment in mice. *Nutrients*. 2022;14:4599.
23. Li L, Dai Y, Ke D, et al. Ferroptosis: new insight into the mechanisms of diabetic nephropathy and retinopathy. *Front Endocrinol*. 2023;14:1215292. doi:10.3389/fendo.2023.1215292
24. Wang Y, Quan F, Cao Q, et al. Quercetin alleviates acute kidney injury by inhibiting ferroptosis. *J Adv Res*. 2021;28:231–243. doi:10.1016/j.jare.2020.07.007
25. Ding L, Dang S, Sun M, et al. Quercetin induces ferroptosis in gastric cancer cells by targeting SLC1A5 and regulating the p-Camk2/p-DRP1 and NRF2/GPX4 Axes. *Free Radic Biol Med*. 2024;213:150–163. doi:10.1016/j.freeradbiomed.2024.01.002
26. Xie R, Zhao W, Lowe S, et al. Quercetin alleviates kainic acid-induced seizure by inhibiting the Nrf2-mediated ferroptosis pathway. *Free Radic Biol Med*. 2022;191:212–226. doi:10.1016/j.freeradbiomed.2022.09.001
27. Abdallah HH, Abd El-Fattah EE, Salah NA, El-Khawaga OY. Rosuvastatin ameliorates chemically induced acute lung injury in rats by targeting ferroptosis, heat shock protein B1, and inflammation. *Naunyn Schmiedebergs Arch Pharmacol*. 2024;398(2):1883–1894. doi:10.1007/s00210-024-03352-9
28. Yang J, Jia Z, Zhang J, et al. Metabolic intervention nanoparticles for triple-negative breast cancer therapy via overcoming FSP1-mediated ferroptosis resistance. *Adv Healthc Mater*. 2022;11:e2102799. doi:10.1002/adhm.202102799
29. Li X, Lu L, Hou W, et al. Epigenetics in the pathogenesis of diabetic nephropathy. *Acta Biochim Biophys Sin*. 2022;54:163–172. doi:10.3724/abbs.2021016
30. Kushwaha K, Kabra U, Dubey R, Gupta J. Diabetic nephropathy: pathogenesis to cure. *Curr Drug Targets*. 2022;23:1418–1429. doi:10.2174/1389450123666220820110801
31. Li A, Yi B, Han H, et al. Vitamin D-VDR (vitamin D receptor) regulates defective autophagy in renal tubular epithelial cell in streptozotocin-induced diabetic mice via the AMPK pathway. *Autophagy*. 2022;18:877–890. doi:10.1080/15548627.2021.1962681
32. Jiang WJ, Xu CT, Du CL, et al. Tubular epithelial cell-to-macrophage communication forms a negative feedback loop via extracellular vesicle transfer to promote renal inflammation and apoptosis in diabetic nephropathy. *Theranostics*. 2022;12:324–339. doi:10.7150/thno.63735
33. Lu Q, Yang L, Xiao JJ, et al. Empagliflozin attenuates the renal tubular ferroptosis in diabetic kidney disease through AMPK/NRF2 pathway. *Free Radic Biol Med*. 2023;195:89–102. doi:10.1016/j.freeradbiomed.2022.12.088
34. Hou Y, Tan E, Shi H, et al. Mitochondrial oxidative damage reprograms lipid metabolism of renal tubular epithelial cells in the diabetic kidney. *Cell Mol Life Sci*. 2024;81:23. doi:10.1007/s00018-023-05078-y
35. Carrillo-Martinez EJ, Flores-Hernandez FY, Salazar-Montes AM, Nario-Chaidez HF, Hernandez-Ortega LD. Quercetin, a flavonoid with great pharmacological capacity. *Molecules*. 2024;29:1000. doi:10.3390/molecules29051000
36. Chellian J, Mak KK, Chellappan DK, Krishnappa P, Pichika MR. Quercetin and metformin synergistically reverse endothelial dysfunction in the isolated aorta of streptozotocin-nicotinamide- induced diabetic rats. *Sci Rep*. 2022;12:21393. doi:10.1038/s41598-022-25739-5
37. Guo X, Wen S, Wang J, et al. Senolytic combination of dasatinib and quercetin attenuates renal damage in diabetic kidney disease. *Phytomedicine*. 2024;130:155705. doi:10.1016/j.phymed.2024.155705
38. Liu F, Feng Q, Yang M, Yang Y, Nie J, Wang S. Quercetin prevented diabetic nephropathy by inhibiting renal tubular epithelial cell apoptosis via the PI3K/AKT pathway. *Phytother Res*. 2024;38:3594–3606. doi:10.1002/ptr.8227
39. Abdou HM, Abd Elkader HAE. The potential therapeutic effects of Trifolium alexandrinum extract, hesperetin and quercetin against diabetic nephropathy via attenuation of oxidative stress, inflammation, GSK-3beta and apoptosis in male rats. *Chem Biol Interact*. 2022;352:109781. doi:10.1016/j.cbi.2021.109781

40. Athyros VG, Katsiki N, Karagiannis A, Mikhailidis DP. Statins can improve proteinuria and glomerular filtration rate loss in chronic kidney disease patients, further reducing cardiovascular risk. Fact or fiction? *Expert Opin Pharmacother*. 2015;16:1449–1461. doi:10.1517/14656566.2015.1053464
41. Laffin LJ, Bruemmer D, Garcia M, et al. Comparative effects of low-dose rosuvastatin, placebo, and dietary supplements on lipids and inflammatory biomarkers. *J Am Coll Cardiol*. 2023;81:1–12. doi:10.1016/j.jacc.2022.10.013
42. Chilbert MR, VanDuyn D, Salah S, Clark CM, Ma Q. Combination therapy of Ezetimibe and Rosuvastatin for Dyslipidemia: current insights. *Drug Des Devel Ther*. 2022;16:2177–2186. doi:10.2147/DDDT.S332352
43. Han E, Kim G, Lee JY, et al. Comparison between atorvastatin and rosuvastatin in renal function decline among patients with diabetes. *Endocrinol Metab*. 2017;32:274–280. doi:10.3803/EnM.2017.32.2.274
44. Kim DH, Choi BH, Ku SK, Park JH, Oh E, Kwak MK. Beneficial Effects of Sarpogrelate and Rosuvastatin in high fat diet/streptozotocin-induced nephropathy in mice. *PLoS One*. 2016;11:e0153965. doi:10.1371/journal.pone.0153965
45. Heeba GH, Ali MAM, El-Sheikh AAK. Rosuvastatin induces renal HO-1 activity and expression levels as a main protective mechanism against STZ-induced diabetic nephropathy. *Medicina*. 2022;58:425. doi:10.3390/medicina58030425
46. Wang H, Liu D, Zheng B, et al. Emerging role of ferroptosis in diabetic kidney disease: molecular mechanisms and therapeutic opportunities. *Int J Biol Sci*. 2023;19:2678–2694. doi:10.7150/ijbs.81892
47. Li Q, Liao J, Chen W, et al. NAC alleviative ferroptosis in diabetic nephropathy via maintaining mitochondrial redox homeostasis through activating SIRT3-SOD2/Gpx4 pathway. *Free Radic Biol Med*. 2022;187:158–170. doi:10.1016/j.freeradbiomed.2022.05.024
48. Chen J, Ou Z, Gao T, et al. Ginkgolide B alleviates oxidative stress and ferroptosis by inhibiting GPX4 ubiquitination to improve diabetic nephropathy. *Biomed Pharmacother*. 2022;156:113953. doi:10.1016/j.biopha.2022.113953
49. Li J, Li L, Zhang Z, et al. Ferroptosis: an important player in the inflammatory response in diabetic nephropathy. *Front Immunol*. 2023;14:1294317. doi:10.3389/fimmu.2023.1294317
50. Cruz-Gregorio A, Aranda-Rivera AK. Quercetin and ferroptosis. *Life*. 2023;13:1730. doi:10.3390/life13081730
51. Zhang L, Wang X, Chang L, et al. Quercetin improves diabetic kidney disease by inhibiting ferroptosis and regulating the Nrf2 in streptozotocin-induced diabetic rats. *Ren Fail*. 2024;46:2327495. doi:10.1080/0886022X.2024.2327495
52. Feng Q, Yang Y, Qiao Y, et al. Quercetin ameliorates diabetic kidney injury by inhibiting ferroptosis via activating Nrf2/HO-1 signaling pathway. *Am J Chin Med*. 2023;51:997–1018. doi:10.1142/S0192415X23500465